A note on the angular correction applied to fracture intensity profiles along drill core

Philippe Davy, Caroline Darcel, Olivier Bour, R. Munier, Jean-Raynald de Dreuzy

A note on the angular correction applied to fracture intensity profiles along drill core

P. Davy,[1] C. Darcel,[2] O. Bour,[1] R. Munier,[3] and J. R. de Dreuzy[1]

Received 25 October 2005; revised 10 July 2006; accepted 7 August 2006; published 30 November 2006.

[1] We derive the angular correction that has to be applied to borehole fracture intensities to recover the actual three-dimensional distribution when the fracture networks have a length distribution. We assume that the fracture intensity is calculated from the fractures that fully transect the core. Because of the length distribution, the classical Terzaghi correction, which involves the cosine of fracture dip, is no longer valid. Solutions have been calculated in the specific case of fractal fracture networks with power law length distribution. We show that the Terzaghi correction may significantly overestimate the frequency of fractures subparallel to the borehole. The correction procedure proposed here was tested on a fracture database recorded at a study site for a repository of spent nuclear fuel located in SE Sweden, with three outcrop maps and three boreholes. A consistency between the dip distributions of outcrops and boreholes was achieved when applying the angular correcting term calculated with the power law length distribution deduced from outcrop maps.

Citation: Davy, P., C. Darcel, O. Bour, R. Munier, and J. R. de Dreuzy (2006), A note on the angular correction applied to fracture intensity profiles along drill core, *J. Geophys. Res.*, *111*, B11408, doi:10.1029/2005JB004121.

1. Introduction

[2] This study is part of an ongoing investigation conducted by the Swedish Nuclear Fuel and Waste management company, SKB, aimed at locating a repository for spent nuclear fuel [*Svensk Kärnbränslehantering* (SKB), 2004, 2005]. Two sites, Forsmark and Simpevarp, are currently under study of which the latter provided data for the work presented here. Knowledge of the spatial distribution of fractures is a key to understanding their influence on hydraulic flow. Unfortunately, most geophysical imagery is "blind" with regard to fractures, and only the largest one are generally detected. Most of the information has to be derived from statistical models whose parameters are defined using limited sampling areas, such as outcrops or wells.

[3] The statistical description of fracture networks still remains a concern for geologists. A challenging task of the last 20-year studies has been to find a solid and rectifiable rationale to the trivial observation that fractures exist everywhere and at a range of sizes. The emergence of fractal models and power law distributions quantifies this fact, and postulates in some ways that small-scale fractures are genetically linked to their larger-scale relatives. This has some consequences on the flow models that can be derived for such distributions [*Bour and Davy*, 1997, 1998; *de Dreuzy et al.*, 2000, 2001a, 2001b; *Renshaw*, 1999]. This also has consequences on how observations obtained at different scales can be linked to each other. This particular point was partly addressed by *Bour et al.* [2002] from outcrops mapped at different scales by *Odling* [1997].

[4] The data set used for the SKB studies consists of large-scale lineament maps covering about 100 km^2, several outcrops of several hundreds of square meters mapped with a fracture trace length resolution down to 0.50 m, and a series of cored boreholes where both fracture orientations and fracture intensities were carefully recorded. Boreholes are an essential complement to surface outcrops as they allow the sampling of horizontal fracture planes that, generally, are severely undersampled in subhorizontal outcrops. Outcrops, on the other hand, provide information on fracture lengths, which is not possible to address from core information alone. However linking outcrops and boreholes is not straightforward for many reasons: the sampling scale is different and some scaling rules have to be applied to relate both fracture distributions; outcrops are two-dimensional (2-D) planes, while boreholes are mostly a 1-D record; outcrops can be affected by superficial fracturing processes that are not representative of the fracturing at depth. For the Simpevarp site, we show that outcrops and boreholes are actually very consistent in terms of fracture density [*Darcel et al.*, 2004], except one point: the orientation distribution. Indeed the difference between outcrops and boreholes cannot be adequately compensated for by the use of the classical Terzaghi orientation correction. Borehole information adjusted using Terzaghi correction predicts much more horizontal fractures than can be justified by outcrop information. This observation cannot easily be explained by superficial fracturing processes since (1) the other terms of the fracture distribution are consistent, (2) no

[1] Geosciences Rennes, UMR 6118 CNRS and University of Rennes I, Rennes, France.
[2] Itasca Consultants, Ecully, France.
[3] Svensk Kärnbränslehantering, Stockholm, Sweden.

0148-0227/06/2005JB004121$09.00

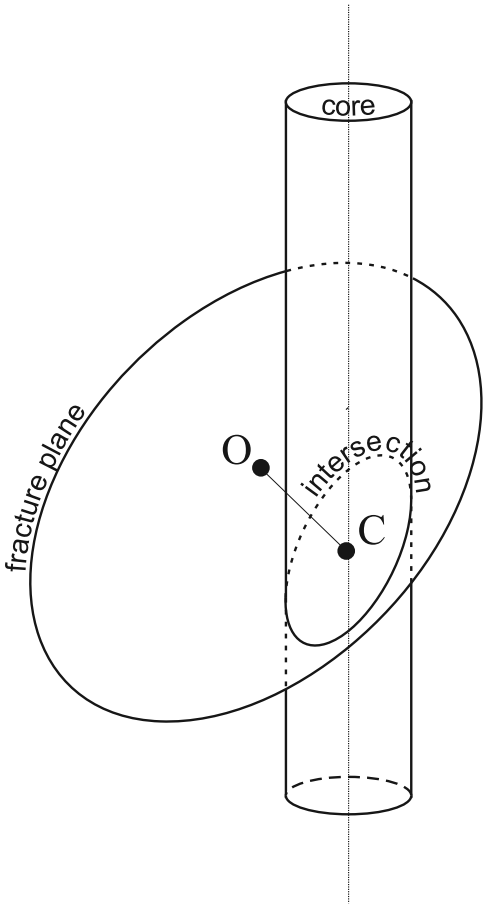

Figure 1. Scheme showing the basic elements of the intersection analysis: the core, the fracture plane and its center *O*, and the intersection ellipse and its center *C*. *C* also belongs to the core axis.

clear depth dependency is observed in boreholes, and (3) superficial processes are likely to produce predominantly horizontal fracturing. Of course, none of the three arguments makes the assessment definitive, but this has nevertheless motivated us to revisit this issue known in the geological community as the Terzaghi correction [*Peacock et al.*, 2003; *Terzaghi*, 1965].

2. Expression of the Core Fracture Intensity

2.1. "Fracturing" Condition

[5] The fracture intensity recorded along a core is a 1-D measure of a 3-D information. The fact that fractures exist at all scales means that part of the information is lost, and that the intersection rules have to be properly defined to understand the meaning of this measure when relating it to the 3D fracture distribution [*Berkowitz and Adler*, 1998; *Darcel et al.*, 2003; *Marrett and Allmendinger*, 1991; *Piggott*, 1997].

[6] In fact, the core is a volume that is likely to contain a very large number of fractures of various lengths. To calculate a scalar value of the fracture intensity, the usual way is to keep only fractures that transect the entire core. Their traces on the borehole walls, which can be detected by high-resolution optical borehole imagery, are continuous. The core diameter thus becomes a lower cutoff of the recorded fracture-length distribution. In the database used, fractures were recorded from both a visual inspection of the cores, and high-resolution optical imagery of the borehole walls. Only fractures whose trace is continuous all around cores and borehole walls have been recorded (as it is illustrated in Figure 1). This condition is a key point of this paper, and most of the consequences derived below stems from it.

2.2. Mathematical Definitions and the Fracture Distribution Model

[7] The second expression needed for calculating the fracture intersection probability is the fracture distribution model. It is quantitatively given by a mathematical expression of the type

$$n_{3D}(L, l, \theta, \varphi, \ldots)\mathrm{d}l\ \mathrm{d}\theta\ \mathrm{d}\varphi\ \mathrm{d}\ldots \tag{1}$$

which is the number of fractures contained in a volume of typical size L, with a length between l and $l + \mathrm{d}l$, orientations in $[\theta, \theta + \mathrm{d}\theta]$ and $[\varphi, \varphi + \mathrm{d}\varphi]$, and a series of other properties that are represented by the cabalistic sign "…". In addition to length and angular characteristics, the expression can include some fracture shape parameters (e.g., eccentricity), which are relevant to the intersection issue. To simplify the notations, we use the general formalism of equation (1) for any subset of parameters; if a parameter is missing, the distribution is calculated for all possible values of this parameter. For instance, the density distribution of fracture orientations, whatever length, writes as

$$n_{3D}(L, \theta, \varphi) = \int_l n_{3D}(L, l, \theta, \varphi)\ dl$$

To limit mathematical complexity, we restrict our analysis to infinitely thin, circular disks. An extension to more complex geometries can be done numerically with the concepts developed below.

[8] Using the appropriate expression for n_{3D} is obviously the key point of this study. In particular, n_{3D} must contain the fundamental scaling relationship that makes it relevant through scale. The simplest model contains two such scaling laws: the fractal density, and the power law length distribution. This has been demonstrated by number of studies (see, e.g., review by [*Bonnet et al.*, 2001]), formalized by *Davy et al.* [1990], and later further elaborated by *Bour et al.* [2002]. Using these scaling assumptions, and assuming that length, density, and orientations are reasonably independent entities, n_{3D} takes the following form:

$$n_{3D}(L, l, \theta, \varphi) = \alpha_{3D}(\theta, \varphi) l^{-a_{3D}} L^{D_{3D}} \tag{2}$$

The power law is limited to small and large fracture lengths, and we denote $l_{\min}$ and $l_{\max}$ the corresponding bounds.

2.3. Fracture Intensity Calculated for Horizontal Fractures

[9] The fracture intensity along the core is calculated as the number of fractures that fully transect the core. To derive the analytical formula, we consider the core as a vertical cylinder of diameter d and height h, and the fracture

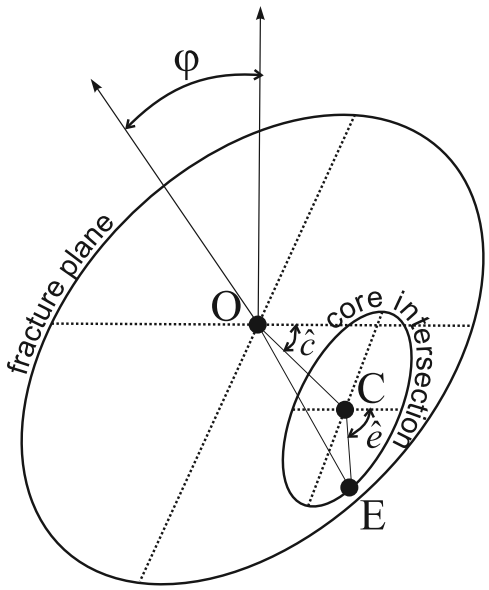

Figure 2. Same scheme as Figure 1 with some useful definitions. O is the fracture center; C is the center of the intersecting ellipse, and $\hat{c}$ the in-plane angle between OC and the horizontal line; E is a point of the intersection ellipse also defined by the angle $\hat{e}$.

as a disk of diameter (equal to fracture length) l and dip φ. We first develop the simple case of horizontal fractures since it constitutes a reference to dipping fractures. The condition for fractures to transect the entire core is simply that the centroid of fracture (point C in Figure 1) is at a distance $(l - d)/2$ of the core axis, or equivalently that C is within a cylinder of base area $\pi\,[(l - d)/2]^2$. For the general case of fractures having a fractal density D_{3D}, the number of fractures that belongs to such a cylinder is

$$n_{1D}(h, l, \theta, \varphi = 0) = h^{D_{3D}-2}\pi\left(\frac{l-d}{2}\right)^2 n_{3D}(\theta, \varphi = 0, l)$$

All these fractures intersect the borehole if their length is larger than d or l_{min} if $l_{min} > d$. The total number of fractures that transect the borehole is then given by

$$n_{1D}(h, \theta, \varphi = 0) = h^{D_{3D}-2} \cdot \alpha_{3D}(\theta, \varphi = 0) \cdot \int_{\max(l_{min}, d)}^{l_{max}} \pi\left(\frac{l-d}{2}\right)^2 l^{-a_{3D}}\,\mathrm{d}l \quad (3)$$

Integrating equation (3) over length gives formally an equation that depends on both the upper and lower bounds of the integral:

$$n_{1D}(h, \theta, \varphi = 0) = \alpha_{3d}(\theta, \varphi = 0)\frac{\pi}{4}h^{D_{3D}-2} \cdot \left[\frac{l^{3-a_{3D}}}{3-a_{3D}} - 2\frac{\mathrm{d}\,l^{2-a_{3D}}}{2-a_{3D}} + \frac{\mathrm{d}^2 l^{1-a_{3D}}}{1-a_{3D}}\right]_{\max(l_{min},\mathrm{d})}^{l_{max}}$$

This ungainly equation can, however, be simplified if one of the bounds of the integral is much larger than the other. In most geological situations, the exponent a_{3D} is larger than 3 [see *Bonnet et al.*, 2001], which makes the lower bound dominate the integral. The self-similar case, where systems appear similar whatever their scale, is obtained for $a_{3D} = D_{3D} + 1$, i.e., for values between 3.5 and 4. Assuming that a_{3D} is much larger than 3 and that l_{min} is smaller than d thus yields the simpler equation

$$n_{1D}(h, \theta, \varphi = 0) = \alpha_{3d}(\theta, \varphi = 0) \cdot \frac{\pi}{2}\frac{h^{D_{3D}-2}d^{3-a_{3D}}}{(a_{3D}-3)(a_{3D}-2)(a_{3D}-1)} \quad (4)$$

Even though we advocate that this case is particularly relevant to geological fracture networks, it is not difficult to calculate similar expressions for exponents a_{3D} smaller than 3 or $l_{min} > d$.

[10] Equation (4) shows that the number of intersecting fractures depends on the core diameter d as $d^{3-a_{3D}}$, meaning that it increases when the core radius decreases for $a_{3D} > 3$. This inverse relationship emphasizes that the number of fractures larger than the core size decreases due to the fracture-length distribution. This is somewhat counterintuitive since the core is a sampling volume, and one could have expected that the larger it is, the larger should be the number of intersecting fractures.

2.4. Fracture Intensity Along Core Calculated for Dipping Fractures (General Considerations)

[11] In the general case of dipping fractures, the expression is more complicated. The intersection with the core is an ellipse whose small and large axes are d and $d/\cos\varphi$, respectively ($d/\cos\varphi$ is thus the minimum fracture length). The intersection center C can be anywhere on the fracture plane if there is no spatial correlation between fractures and the well. The condition for having the core fully transected by the fracture (i.e., the intersection ellipse within the disk) varies with the position of C (see Figure 2). If OC is horizontal, the distance $\overline{OC}$ must be smaller than $(l - d)/2$, as in the horizontal fracture case. If OC is in the dip direction ($\hat{c} = 90°$, see Figure 2), the distance $\overline{OC}$ must be smaller than $(l\cos\varphi - d)/2$. If C does not belong to these particular lines of the fracture plane, the full transecting condition is $\overline{OE} < l$, with E the point of the intersecting ellipse that is the farthest from the fracture center O. E is given by

$$\overline{OE}^2 = \overline{OC}^2 + \overline{CE}^2 + 2\overline{OC} \cdot \overline{CE} \cdot \cos(\hat{c} - \hat{e})$$

A parameterized solution can be derived, but the expression is complicated and cannot be easily integrated over the whole fracture distribution to calculate the probability of having the fracture fully transecting the core.

[12] The results presented in the following paragraphs are derived from Monte Carlo simulations where both the fracture length l and center are stochastically drawn from probability distributions. Following the previous reasoning, only fractures whose center is at a distance less than $(l - d)/2$ can fully transect the core. Moreover if this distance condition is fulfilled, the transecting probability is 1 for flat fractures. We thus restrict the calculation to fracture centers randomly contained in the cylinder centered on the core axis, and of radius $(l - d)/2$. This comes to calculate the transecting probability normalized by that of flat fractures, that is the actual angular correcting factor called $P(\varphi)$ in the following paragraphs.

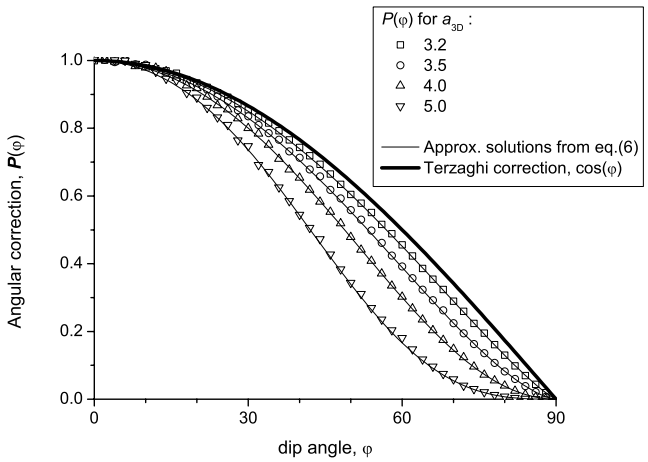

Figure 3. Angular correction for a fracture of dip φ. Fracture centers are chosen so that an equivalent horizontal fracture necessarily transects the core (i.e., the distance between the fracture center and the core axis is less than $(l - d)/2$, with l and d the fracture and core diameter, respectively). The symbols correspond to power law fracture size distribution with exponents a_{3D} of 3.2 (squares), 3.5 (circles), 4.0 (triangles) and 5.0 (inverted triangles). The thin lines are approximated solutions calculated with equation 6. The thick solid line is the Terzaghi correction $P(\varphi) = \cos\varphi$.

[13] In practice, the fracture centers are chosen at random within the abovementioned cylinder, which is consistent with the assumption that the core position is not correlated with the fracture network. Once the fracture length and position are drawn from the probability distributions, the program calculates the number of fractures that fully transect the core and thus derives the transecting probability as a function of the dip angle φ.

2.5. Fracture Intensity Along Core Calculated for a Power Law Length Distribution Without Lower Limit

[14] Figure 3 shows the angular correction factor $P(\varphi)$ calculated for fractures following power law length distributions with l_{min} smaller than d. If the exponent a_{3D} is 3 (this is also valid for any exponent smaller than 3), the transecting probability is the classical Terzaghi correction $\cos\varphi$. For larger exponents, the transecting probability decreases much faster with φ than the Terzaghi correction. The difference can be quite large: for instance, for $a_{3D} = 4$, the intersection probability is 1.6 smaller than the classical Terzaghi correction at $\varphi = 60°$, 2.3 at 70° and 4.5 at 80°. The reason for this discrepancy is twofold: the length distribution is dominated by its lower bound, and this bound increases with dip since oblique fractures need to be larger than perpendicular ones.

[15] We have looked for a parameterized solution of $P(\varphi)$. We first point out that the function mostly depends on $(\cos\varphi)^{a_{3D}-2}$ as it is illustrated in Figure 4. To decrease further the scattering, we fit each curve by a second-order polynomial function of the form

$$P(\chi) = a_1\chi + a_2\chi^2, \text{ with } \chi = (\cos\varphi)^{a_{3D}-2} \quad (5)$$

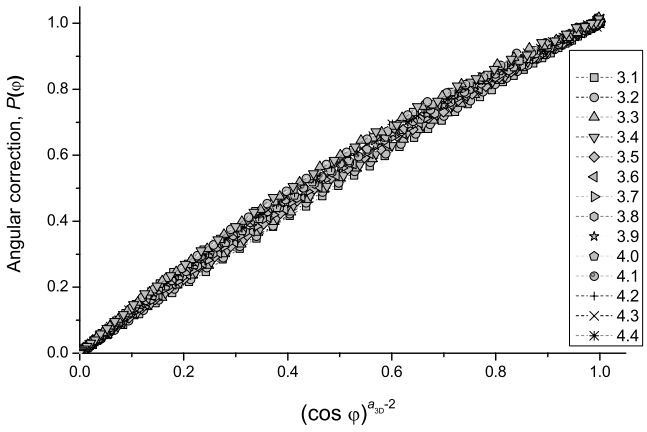

Figure 4. Same as figure 3, except the horizontal axis that is $(\cos\varphi)^{a_{3D}-2}$. The scattering observed in Figure 3 appears to be significantly reduced.

The coefficients a_1 and a_2 depend on a_{3D} only. They present a remarkable symmetry with $a_1 = 1 - a_2$, which simplifies the previous χ equation as $P(\chi = (\cos\varphi)^{a_{3D}-2}) = \chi\,(1 - a_2\,(1 - \chi))$; a_2 (and thus $a_1 - 1$) was also found to be proportional to $a_{3D} - 3$, with a proportionality coefficient that varies as (see Figure 5)

$$a_* = \frac{a_1 - 1}{a_{3D} - 3} = -\frac{a_2}{a_{3D} - 3} \text{ if } a_{3D} < 3.6,$$
$$a_* = 0.27*(4.7 - a_{3D}), \text{ if } a_{3D} > 3.6,$$
$$a_* = \frac{3}{38}*(7.4 - a_{3D})$$

Eventually, we find that $P(\varphi)$ can be well approximated by the following expression whatever $a_{3D} > 3$:

$$P_{approx}(\varphi) = \cos\varphi^{a_{3D}-2}\left(1 + \frac{3}{38}*(a_{3D} - 3)(7.4 - a_{3D}) \cdot \left(1 - \cos\varphi^{a_{3D}-2}\right)\right) \quad (6)$$

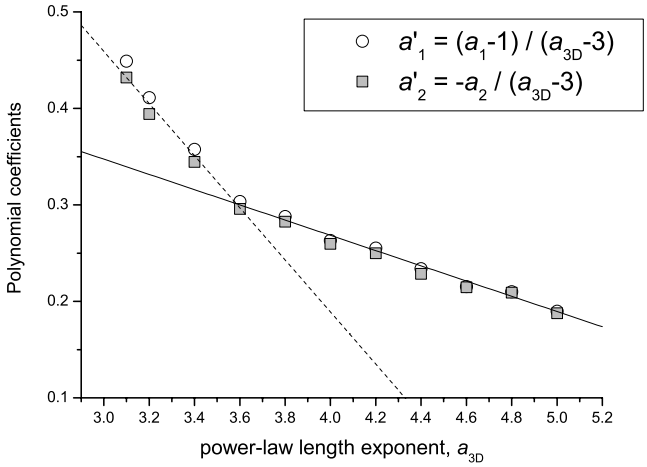

Figure 5. Dependency of the reduced polynomial coefficients $a_1'(= (a_1 - 1)/(a_{3D} - 3))$ and $a_2'(= -a_2/(a_{3D} - 3))$ with the power law exponent a_{3D}. The parameters a_1 and a_2 are defined in equation (5).

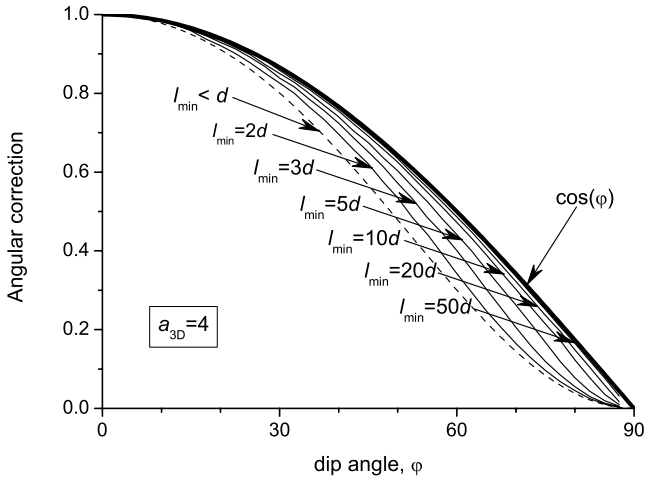

Figure 6. Transecting probability for fractures following a power law distribution with an exponent $a_{3D} = 4$ and different values of l_{min}. As in Figure 3, the probability is calculated for fracture whose center is at a distance less than $(l - d)/2$ of the core axis.

The difference between $P(\varphi)$ and $P_{approx}(\varphi)$ is less than 0.01 whatever the value of a_{3D} (Figure 3). It is not necessary to consider the case of $3 < a_{3D} < 3.6$, which was previously invoked, because the correcting term (3/38*...) becomes negligible when a_{3D} approaches 3. For $a_{3D} < 3$, the Terzaghi correction factor ($P(\varphi) = \cos\varphi$) applies.

[16] By mixing equations (4) and (6), we can now derive the general stereological formula that gives n_{1D} as a function of n_{3D} for $a_{3D} > 3$ and $l_{min} < d$:

$$n_{1D}(h,\theta,\varphi) = \alpha_{3d}(\theta,\varphi)\frac{\pi}{2}\frac{h^{D_{3D}-2}d^{3-a_{3D}}\cos\varphi^{a_{3D}-2}}{(a_{3D}-3)(a_{3D}-2)(a_{3D}-1)} \cdot \left(1-\frac{3}{38}*(a_{3D}-3)(7.4-a_{3D})\left(1-\cos\varphi^{a_{3D}-2}\right)\right) \quad (7)$$

We wish to stress two points:

[17] 1. The condition of fully intersecting the core must not be taken in its strictest sense. Expressions similar to equation (7) can be derived for fractures intersecting only a portion of the core. The correcting term in $\cos\varphi^{a_{3D}-2}$ prevails as long as the criterion is independent on the fracture dip φ; only the proportional coefficient is changed, with the consequence of increasing n_{1D} if the proportion of broken core decreases.

[18] 2. The fracture intensity n_{1D} contains two scales: the core radius and the borehole length. The former is directly related to the parameters of the fracture length distribution; the latter depends on the fractal dimension of the fracture network D_{3D}. This fixes the type of scaling information that is contained in such measurements.

2.6. Fracture Intensity Along Core for Power Law Length Distribution With Nonnegligible Lower Bound

[19] Assessing the lower bound of the power law model is an open issue with important consequences for microfracture distribution. Here we consider the possibility of having l_{min} much larger than d. Figure 6 shows the angular correction factor $P(\varphi)$ for different values of the ratio d/l_{min} with a power law exponent of 4. As l_{min} increases, the dip correction goes back to the Terzaghi correction. For $l_{min} = 3d$, the discrepancy with the Terzaghi correction is already reduced by about 50%. For $l_{min} = 10d$, the Terzaghi correction applies.

[20] Thus, if l_{min} is significantly larger than the borehole diameter, the stereological rule is given by both equation (3) and the Terzaghi correction:

$$n_{1D}(h,\theta,\varphi) = \alpha_{3d}(\theta,\varphi)\frac{\pi}{4}h^{D_{3D}-2}l_{min}^{3-a_{3D}}\left(\frac{1}{a_{3D}-3} - \frac{2}{a_{3D}-2}*\frac{d}{l_{min}} + \frac{1}{a_{3D}-1}\left(\frac{d}{l_{min}}\right)^2\right)\cos\varphi$$

3. Ground Truthing

[21] The Simpevarp investigation has provided a record of fractures in 12 boreholes, the detailed mapping of four outcrops, and three region-scale lineament maps, all with a very high resolution not reached in previous studies. Drill cores are oriented in three dimensions by the use of borehole video imagery combined with borehole deviation measurements. We use the three flat-lying outcrops to test the theme argued for in this paper and three boreholes.

[22] *Darcel et al.* [2004] analyzed the fracture distribution in the Simpevarp area, using graphs such as shown in Figure 7. They concluded that the parameters are mostly dependent on lithology, with power law length exponents that vary from $a_{2D} = 2.15$ in granitoid lithology to $a_{2D} = 3$ in dioritic rocks (or equivalently $a_{3D} = 3.15$, and $a_{3D} = 4$, respectively). The core fracture intensity also varies with lithology, from three to seven fractures per meter in granitoids to 10–20 in dioritic rocks. These values are consistent with fracture densities measured on outcrops, once the scaling correction is applied via equation (7).

[23] The distribution of fracture dips is shown in Figure 8 for both boreholes and outcrop maps. In boreholes, the

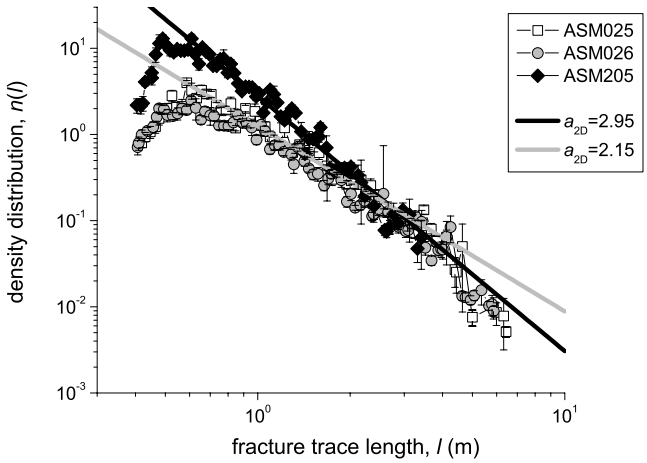

Figure 7. Length distribution calculated for the outcrops ASM025 (open square), ASM026 (gray circle), and ASM0205 (solid diamond). Between 0.6 and 7 m, the density distributions are well fitted by power laws, whose exponents a_{2D} are 2.95 (ASM0205, black straight line) and 2.15 (ASM025 and ASM025, gray straight line).

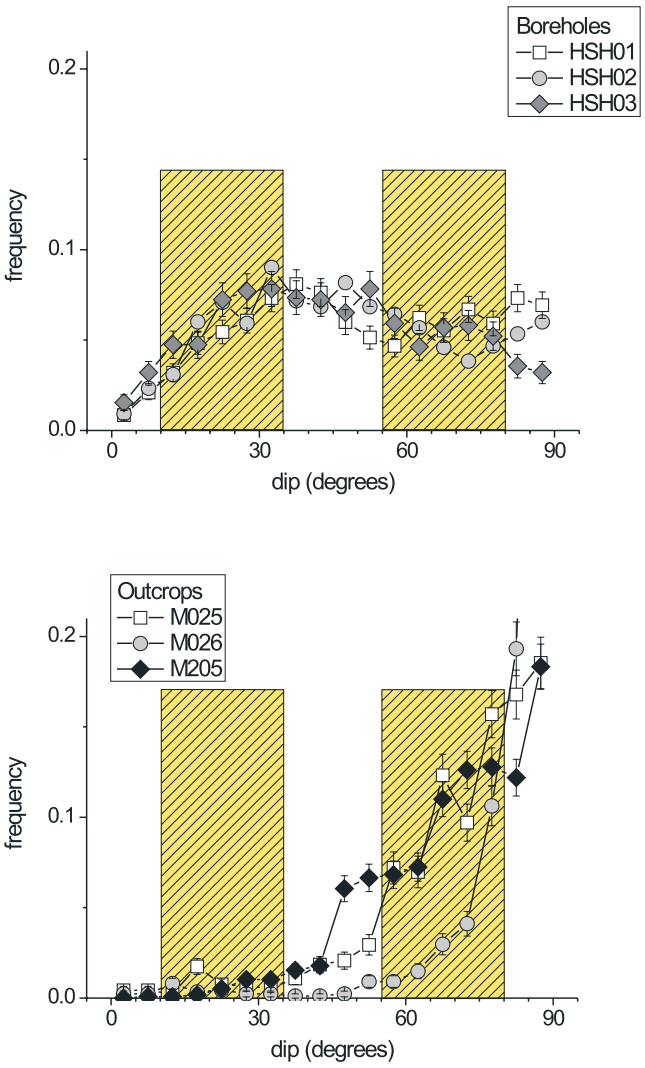

Figure 8. Distributions of fracture dips calculated for (top) boreholes and (bottom) outcrop maps. The hatched squares show the orientation ranges that we use to compare distributions (see text).

distribution is wide, with a peak at around 35–40° and a significant number of subvertical fractures (whose probability of intersecting the borehole is very small). In contrast, most of the fractures encountered in outcrops are about vertical.

[24] As argued before, the angular correction to the orientation distributions consists in dividing the probability distribution by the cosine (vertical borehole) or sine (horizontal plane) of the fracture dips. The procedure is obviously biased for strictly horizontal or strictly vertical fractures, for which the correction factor can take infinite (or extremely large) values. Rather than introducing an ambiguous threshold for the correction factor, we compared outcrops and boreholes in a range of dip orientation that is not unduly affected by this bias (hatched zones in Figure 8). We take the ratio between the two populations (10–35° versus 55–80°) as a first-order indicator of the orientation distribution. The data, with and without the Terzaghi correction, are presented in Figure 9. The Terzaghi correction improves the data consistency by decreasing this

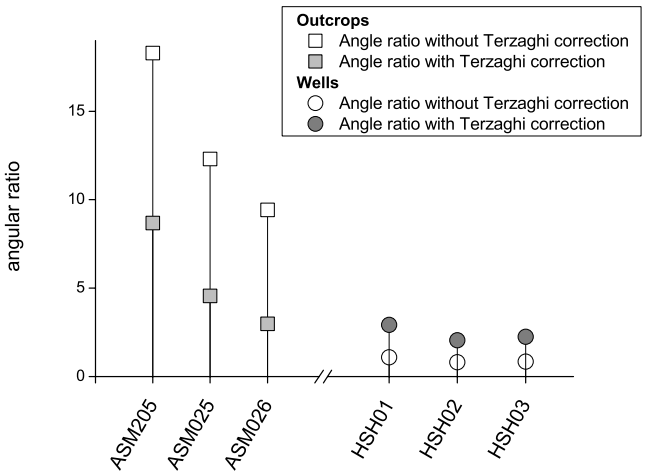

Figure 9. Angular ratio (vertical axis) is a fracture number ratio between two populations whose dip is 50–70° on the one hand and 20–40° on the other hand. Open symbols with black contour represent the observed ratio for both outcrops and boreholes, while colored symbols (squares for outcrops and circles for boreholes) represent the population ratio calculated when applying the Terzaghi correction.

angular ratio for outcrops and increasing it for boreholes. Both granitoid outcrops, ASM025 and ASM026, are consistent with borehole data using this correction. However, the last outcrop ASM205, for which a large exponent a_{2D} of 2.95 has been measured, remains much larger than the borehole ratios, which means that the number of horizontal fractures is abnormally large for boreholes (or conversely the number of vertical fractures is abnormally large for outcrops). We now check if the correction developed in the previous paragraph (equation (7)) improves the consistency between the fracture dip distribution of outcrops and boreholes. Note that this correction has been applied by assuming that strike and dip are independent variables. Figure 10

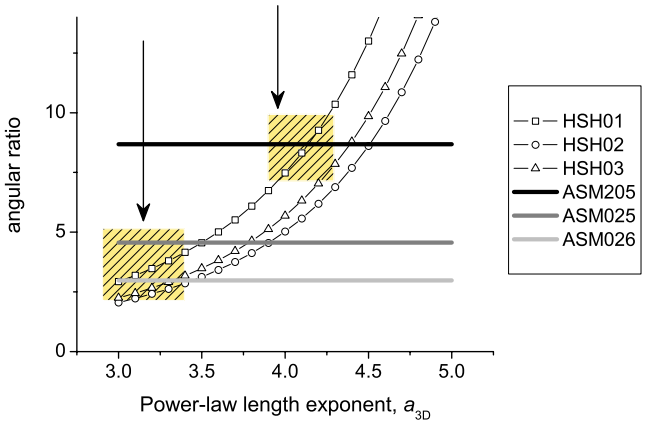

Figure 10. Angular ratio (see Figure 9) recalculated according to equation (6) for boreholes, and to the classical Terzaghi correction for outcrops. Only borehole dip distribution depends on the exponent of the length distribution. The two hatched boxes indicate the range of power law exponents that ensure the angular consistency between boreholes and outcrops. The black arrows indicate the power law length exponents measured from the outcrop fracture trace maps.

shows the borehole correction for different power law exponents. The consistency between outcrops and boreholes is obtained when the outcrop ratio is equal to the borehole ratio. We observe that the consistency between boreholes and outcrops can be obtained for a_{3D} of about 3–3.5 for outcrops ASM025 and ASM026, and a_{3D} of about 4–4.5 for ASM205, which is consistent (considering both the uncertainty on this angular ratio) with the power law length exponents measured for these outcrops. This tends to prove that the outcrop ASM205, which would have appeared inconsistent with boreholes if applying the classical Terzaghi correction, is actually consistent if the length distribution is a power law with an exponent of about 4 and a lower bound smaller than 80mm (the core diameter).

4. Conclusion

[25] The objective of this paper is to discuss the fracture orientation consistency between borehole fracturing data and outcrop fracture maps. This is worth being revisited considering the importance of assessing a sound fracture orientation distribution for some sensitive applications such the permeability model of potential nuclear waste disposals or production models for oil extraction.

[26] The rationale is based on two basic observations:

[27] 1. The fracture information in boreholes depends on the core diameter if the fracturing intensity profile along core is defined from fractures that essentially transect the core.

[28] 2. The probability of intersecting a core depends on the distributions of both fracture lengths and orientations.

[29] On the basis of these hypotheses, we have recalculated the probability distribution of fractures along core as a function of the fracture dip distribution and of the fracture length distribution. The particular, but geologically relevant, case of a power law fracture length distribution was specifically investigated. If the power law length exponent a_{3D} is larger than 3, the factor correcting fracture intensity is no longer defined by the classical Terzaghi term $\cos\varphi$ [*Terzaghi*, 1965], but a coefficient that depends on a_{3D} and $(\cos\varphi)^{a_{3D}-2}$, φ being the fracture dip for vertical boreholes (or the equivalent in the borehole referential for nonvertical boreholes). The correcting factor for $a_{3D} > 3$ predicts that the probability of intersecting subvertical fractures in boreholes decreases considerably when increasing a_{3D}.

[30] If the power law exponent is smaller than 3, or if the lower bound of the power law length distribution is much larger (i.e., > 5–10x) than the core diameter, the Terzaghi coefficient $\cos\varphi$ applies.

[31] We have applied the modified angular correction to the fracture data obtained from the mapping in the Simpevarp area (Sweden). Even if we cannot fully guarantee that the fracturing distribution is similar in borehole and outcrops (no depth effect for instance), we do find that the consistency between outcrops and boreholes is ensured when applying the modified angular correction, while it was not with the classical Terzaghi correction. Moreover, the power law length exponents predicted by our angular consistency condition are about the same as those calculated from the outcrop length distributions. This result suggests in particular that the lower limit of the power law length distribution is smaller than core size.

[32] This study also emphasizes that borehole information should be used with great care when used to reveal 3-D fracture distribution, and that the statistical consistency between information at different scales is model-dependent.

References

Berkowitz, B., and P. Adler (1998), Stereological analysis of fracture network structure in geological formations, *J. Geophys. Res.*, *103*, 15,339–15,360.

Bonnet, E., O. Bour, N. E. Odling, P. Davy, I. Main, P. Cowie, and B. Berkowitz (2001), Scaling of fracture systems in geological media, *Rev. Geophys.*, *39*, 347–384.

Bour, O., and P. Davy (1997), Connectivity of random fault networks following a power law fault length distribution, *Water Resour. Res.*, *33*, 1567–1584.

Bour, O., and P. Davy (1998), On the connectivity of three-dimensional fault networks, *Water Resour. Res.*, *34*, 2611–2622.

Bour, O., P. Davy, C. Darcel, and N. Odling (2002), A statistical scaling model for fracture network geometry, with validation on a multiscale mapping of a joint network (Hornelen Basin, Norway), *J. Geophys. Res.*, *107*(B6), 2113, doi:10.1029/2001JB000176.

Darcel, C., O. Bour, and P. Davy (2003), Stereological analysis of fractal fracture networks, *J. Geophys. Res.*, *108*(B9), 2451, doi:10.1029/2002JB002091.

Darcel, C., P. Davy, O. Bour, and J. R. de Dreuzy (2004), Alternative DFN model based on initial site investigations at Simpevarp, *R-04-76*, 107 pp., Svensk Kärnbränslehantering, Stockholm.

Davy, P., A. Sornette, and D. Sornette (1990), Some consequences of a proposed fractal nature of continental faulting, *Nature*, *348*, 56–58, doi:10.1038/348056a0.

de Dreuzy, J.-R., P. Davy, and O. Bour (2000), Percolation parameter and percolation-threshold estimates for three-dimensional random ellipses with widely scattered distributions of eccentricity and size, *Phys. Rev. E*, *62*, 5948–5952, doi:10.1103/PhysRevE.62.5948.

de Dreuzy, J., P. Davy, and O. Bour (2001a), Hydraulic properties of two-dimensional random fracture networks following a power law length distribution: 1. Effective connectivity, *Water Resour. Res.*, *37*, 2065–2078.

de Dreuzy, J.-R., P. Davy, and O. Bour (2001b), Hydraulic properties of two-dimensional random fracture networks following a power law length distribution: 2. Permeability of networks based on lognormal distribution of apertures, *Water Resour. Res.*, *37*, 2079–2096.

Marrett, R., and N. E. Allmendinger (1991), Estimates of strain due to brittle faulting: Sampling of fault populations, *J. Struct. Geol.*, *13*, 735–738.

Odling, N. E. (1997), Scaling and connectivity of joint systems in sandstones from western Norway, *J. Struct. Geol.*, *19*, 1257–1271, doi:10.1016/S0191-8141 (97)00041-2.

Peacock, D. C. P., S. D. Harris, and M. Mauldon (2003), Use of curved scanlines and boreholes to predict fracture frequencies, *J. Struct. Geol.*, *25*, 109–119, doi:10.1016/S0191-8141 (02)00016-0.

Piggott, A. (1997), Fractal relations for the diameter and trace length of disc-shaped fractures, *J. Geophys. Res.*, *102*, 18,121–18,126.

Renshaw, C. E. (1999), Connectivity of joint networks with power law length distributions, *Water Resour. Res.*, *35*, 2661–2670.

Svensk Kärnbränslehantering (SKB) (2004), Preliminary site description. Simpevarp area, version 1.1, *SKB R-Rep. R-04-15*, 399 pp., Stockholm.

Svensk Kärnbränslehantering (SKB) (2005), Preliminary site description Forsmark area, version 1.2, updated, *SKB R-Rep. R-05-18*, 752 pp., Stockholm.

Terzaghi, R. D. (1965), Sources of errors in joint surveys, *Geotechnique*, *15*, 287–304.

O. Bour, P. Davy, and J. R. de Dreuzy, Geosciences Rennes, UMR 6118 CNRS and University of Rennes I, Campus de Beaulieu, F-35042 Rennes Cedex, France. (phillipe.davy@univ-rennes1.fr)

C. Darcel, Itasca Consultants S. A., Groupe HCItasca, 64 Chemin des Mouilles, F-69130 Ecully, France.

R. Munier, Svensk Kärnbränslehantering AB, Box 5864, SE-102 40 Stockholm, Sweden.